

Novel Crosslinked Nonlinear Optical Materials Based on Cellulose Diacetate

Limin Zhou, Qiang Xu, Dening Wang

School of Materials Science and Engineering, East China University of Science and Technology, 130 Meilong Road, Shanghai 200237, China

Received 23 January 2005; accepted 22 March 2005

DOI 10.1002/app.21947

Published online 9 February 2006 in Wiley InterScience (www.interscience.wiley.com).

ABSTRACT: Preparation of second-order nonlinear optical (NLO) materials based on cellulose diacetate and melamine derivatives was attempted. The NLO chromophore DR19 was incorporated into the crosslinking network resulting from the reaction of cellulose diacetate with trimethylolmelamine or hexamethylolmelamine. The poled and cured NLO materials exhibited electrooptic coefficient (r_{13}) values of 1.11 or 1.03 pm/V, respectively, at a laser wavelength of 1550 nm, a modulation frequency of 12.7 kHz. The r_{13} values decreased to 80 or 81.5% of the initial values after 4 days.

The laser transmission loss was 0.50 or 0.44 db. The crosslinking materials showed better temporal stability than that of host/guest type materials, and 73% of the initial r_{13} value remained after keeping the NLO film at 100°C for 15 h. No evident weight loss was found below 250°C. © 2006 Wiley Periodicals, Inc. *J Appl Polym Sci* 100: 2832–2837, 2006

Key words: cellulose diacetate; trimethylolmelamine; hexamethylolmelamine; nonlinear optical material; chromophore

INTRODUCTION

Development of optical communications led to interest in research on nonlinear optical (NLO) materials, especially those based on organic polymers, which can possess the advantages of large susceptibility, high laser damage threshold, faster response time, versatility of the molecular structure, and good mechanical performance.¹ The molecular structure of second-order NLO materials should not have any center of symmetry. The NLO chromophores contained in an amorphous polymer orient in an electric field at about the glass-transition temperature (T_g) of the polymer, and the poled material should then be cooled down in the electric field to stabilize the orientation of the poled chromophores. The incorporation of NLO chromophores into a polymer occurs in one of four ways: to form a host/guest system, as a side-chain polymer, in the main chain of the polymer, and to form a crosslinking network.² For a useful NLO material, chemical and physical stability are required. Therefore, most researchers focused on polymers with a high T_g or crosslinking polymers.

Cellulose derivatives³ are rigid and their molecular chains are not easily moved because of glucose units. Moreover, hydroxyl groups are attached to the molecules of cellulose derivatives and can react with some

crosslinking agents to form a crosslinking network. Therefore, cellulose derivatives might be useful for preparing NLO materials.

Melamine derivatives were widely used for lighting, coating, and decorating because of their good transparency.⁴ The preparation of the materials based on melamine derivatives involved a condensation reaction, which can provide an attractive way for the formation of a crosslinking polymer network⁵ to stabilize the oriented NLO chromophores by decreasing their mobility. In addition, melamine-based polymers can show low optical loss and high T_g . Jeng et al.⁶ and Hsiue et al.⁷ reported that methylated hexamethylolmelamine (HMM) was used for preparing NLO polymer materials.

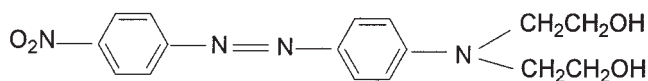
In the present work, the preparation of second-order NLO materials based on cellulose diacetate (CDA) and chromophore DR19 was attempted by using trimethylolmelamine (TMM) or HMM as a crosslinking agent. The crosslinking structure was characterized and some properties of the materials were studied.

EXPERIMENTAL

Materials

CDA $\{[C_6H_7O_2(OCOCH_3)_{2.4}(OH)_{0.6}]_n\}$ formula from Mark et al.³ and *N,N*-dihydroxyethylaniline were industrial products available from Shanghai Chemical Reagent Co. and Haineng Chemical Co., respectively. Other starting materials and solvents were reagent grade and used as received.

Correspondence to: D. Wang (wangdening@hotmail.com).



Scheme 1 The chemical structure of DR19.

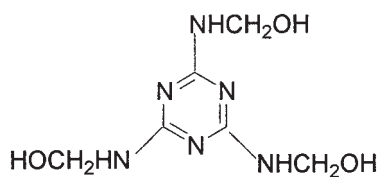
Synthesis

Chromophore DR19

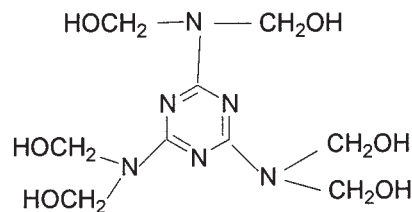
The chemical structure of DR19 is provided in Scheme 1. *p*-Nitroaniline (13.8 g) and HCl (22 mL, concentration = 37 wt %) were put into water (50 mL) to form a solution. The solution of *p*-nitroaniline was poured under strong stirring into a beaker containing water (300 mL) and trash ice (300 g), and fine *p*-nitroaniline precipitates formed immediately. Sodium nitrite (7.0 g) dissolved in water (30 mL) was added dropwise into the *p*-nitroaniline solution at 0°C for 10 min. After 40 min, carbamide (1.0 g) was added for 20 min. Then, the solution was neutralized by saturated sodium acetate solution until the pH value reached 6–7. *N,N*-dihydroxyethylaniline (18.1 g) was added to the reaction system over 3 h. Thereafter, sodium chloride (100 g) was added. Finally, a deep red solid (22.6 g) was obtained by filtration and recrystallization twice from pure ethanol. Its melting and decomposition temperatures were 212–215 and 290°C, respectively. The results of the elemental analysis are as follows: ANAL. calcd for $C_{16}H_{18}N_4O_4$: C, 58.18%; H, 5.45%; N, 16.97%. Found: C, 58.22%; H, 5.41%; N, 17.26%. $^1\text{H-NMR}$ (DMSO- d_6 , δ): 8.31 (2H, d, $J_{\text{H-H}} = 8.5$ Hz), 7.95 (2H, d, $J_{\text{H-H}} = 9.0$ Hz), 7.81 (2H, d, $J_{\text{H-H}} = 8.2$ Hz), 6.93 (2H, d, $J_{\text{H-H}} = 8.2$ Hz), 4.90 (2H, s), 3.61 (8H, s).

TMM

The chemical structure of TMM is shown in Scheme 2. Formaldehyde (160.0 g, concentration = 37 wt %) was neutralized with triethanol amine (2.0 g) until the pH value reached 8. Then, water (100 g) and melamine (75.0 g) were added gradually and the solution was heated to 78°C. After 30 min it was cooled to room temperature, stored for 24 h, and filtrated. TMM (40.0 g) was obtained after the filter cake was washed with water several times and dried below 50°C under a vacuum. The elemental analysis results are as follows: ANAL. calcd for $C_6H_{12}N_6O_3$: C, 33.33%; H, 5.56%; N,



Scheme 2 The chemical structure of TMM.



Scheme 3 The chemical structure of HMM.

38.89%. Found: C, 33.12%; H, 5.47%; N, 39.02%. $^1\text{H-NMR}$ (DMSO- d_6 , δ): 5.45 (H, t, $J_{\text{H-H}} = 7.2$ Hz), 5.01 (2H, d, $J_{\text{H-H}} = 7.3$ Hz).

HMM

The chemical structure of HMM is provided in Scheme 3. Formaldehyde (152.2 g, concentration = 37 wt %) was mixed with water (24.2 g) and then neutralized with the solution of sodium hydroxide in water (concentration = 10%) until the pH value reached 9.0. Melamine (23.6 g) was added gradually, and the solution was heated to 60°C and maintained at this temperature for 3–4 h. It was then cooled to room temperature and filtrated. HMM (42.7 g) was collected after the filter cake was washed with water several times and dried below 50°C under a vacuum. The results of the elemental analysis are as follows: ANAL. calcd for $C_9H_{18}N_6O_6$: C, 35.29%; H, 5.89%; N, 27.22%. Found: C, 35.04%; H, 5.73%; N, 27.45%. $^1\text{H-NMR}$ (DMSO- d_6 , δ): 5.45 (H, t, $J_{\text{H-H}} = 7.30$), 5.0 (2H, d, $J_{\text{H-H}} = 7.29$).

Preparation of NLO polymer solutions

CDA, TMM, and HMM were dissolved in *N,N*-dimethylformamide (DMF) to form a solution of CDA in DMF with a concentration of 8.0 wt %, a solution of

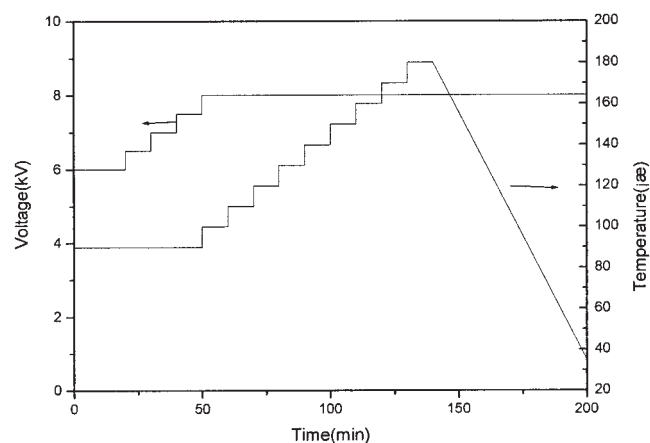


Figure 1 The process of stagewise poling and curing of the film.

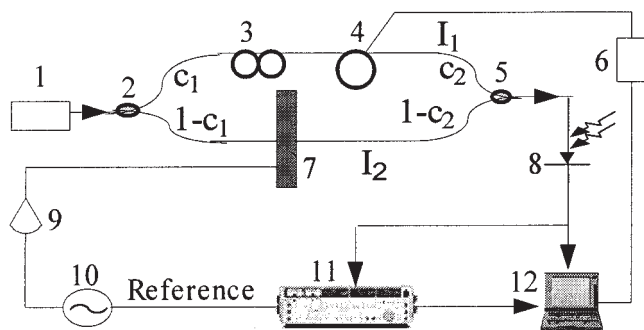


Figure 2 The experimental setup to measure the electrooptic coefficient (r_{13}): 1. laser, 2. coupler 1, 3. polarization controller, 4. piezoelectric tensor, 5. coupler 2, 6. DC voltage source, 7. polymer sample, 8. detector, 9. amplifier, 10. wave-form generator, 11. lock-in amplifier, 12. computer.

TMM in DMF with a concentration of 20.0%, and a solution of HMM in DMF with a concentration of 20.0%, respectively. Each solution was filtered to remove impurities. The NLO polymer solution containing 25% DR19 and without any crosslinking agent (sample I) was prepared by mixing 0.125 g of DR19 and 4.7 g of a solution of CDA in DMF. The NLO polymer solution containing TMM and 25% DR19 (sample II) was prepared by mixing 0.125 g of DR19, 0.875 g of the solution of TMM in DMF, and 2.5 g of the solution of CDA in DMF. The NLO polymer solution containing HMM and 25% DR19 (sample III) was prepared by mixing 0.125 g of DR19, 0.875 g of the solution of HMM in DMF, and 2.5 g of the solution of CDA in DMF.

Poling and curing of NLO films

Each of the described solutions was spin coated on an ITO glass plate to form a film with a thickness of about 3 μm . The film was dried at 75°C under a vacuum for 24 h and then subjected to corona poling from 6.0 to 8.0 kV and curing from 80 to 180°C. The poling and

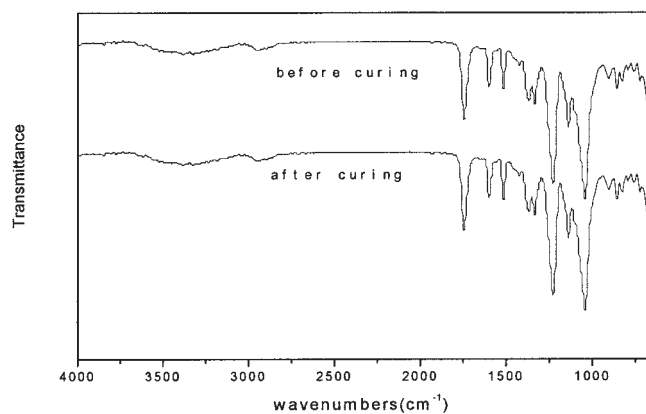


Figure 3 The IR spectra of sample I.

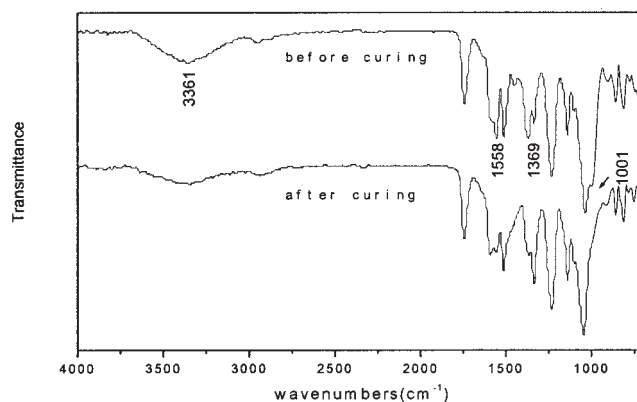


Figure 4 The IR spectra of sample II.

curing process continued about 150 min as shown in Figure 1. The film was then cooled to room temperature in an electric field for about 60 min.

Measurements

The weight loss of the samples was determined by using a WRT-2P thermogravimetric analysis (TGA) instrument at a heating rate of 10°C/min. A Nicolet AVATAR 360 FTIR spectrometer was used to characterize the chemical composition of the NLO materials. Elemental analysis was carried out with a Heraeus CHN-RQPID instrument. The $^1\text{H-NMR}$ data were measured with a Bruker DRX-500. The dielectric relaxation of the NLO materials was tested with a CONCEPT 40 dielectric spectrometer (Novercontrol GmbH). The transmission loss was measured with an Anritsu MS9710B optical spectrum analyzer.

For measuring the susceptibility (χ) value,² the Pockels effect was determined with a Mach-Zehnder interferometer prepared by Shanghai Jiaotong University to obtain the electrooptic coefficient (r_{13}). The r_{13} values of the materials were found with a laser wavelength of 1550 nm and a modulation frequency of 12.7 kHz. The schematic diagram of the experiment setup

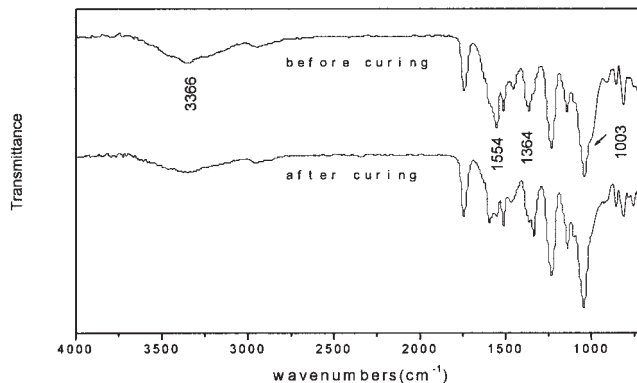


Figure 5 The IR spectra of sample III.

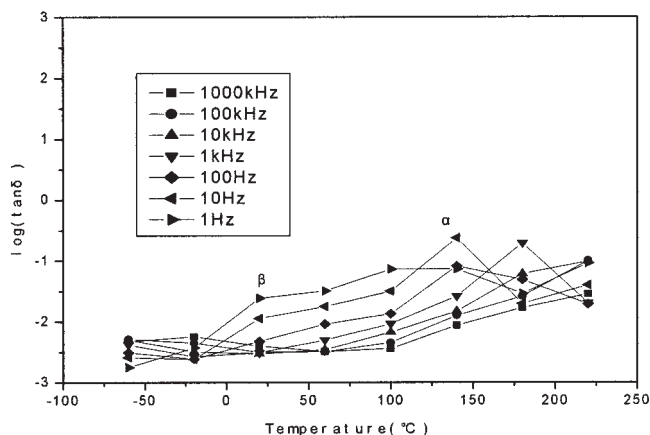


Figure 6 The temperature dependence of $\log(\tan \delta)$ for sample I.

is shown in Figure 2. The main part is an optical fiber Mach-Zehnder interferometer consisting of two fiber couplers (points 2 and 5). A piezoelectric tensor phase modulator is put in one of the two light paths between the two couplers to adjust the phase difference. The polarization controller (point 3) is used to control the state of polarization of the interference laser beam. The polymer film is inserted perpendicularly into the other light path (point 7). The optical signal output is detected with a PIN diode and a lock-in amplifier (point 11).

The r_{13} was calculated by the equation

$$r_{13} = \frac{2I_{m0}\lambda}{\pi n^3 V_{m0}(I_{\max} - I_{\min})} \quad (1)$$

where I_{m0} is the electric current modulation intensity; λ is the wavelength; n is the refractive index of the film; V_{m0} is the modulation voltage; and I_{\max} and I_{\min} are the maximum and minimum of the output light intensity, respectively.

RESULTS AND DISCUSSION

Characterization of samples before and after curing

Because of the hydroxyl groups attached to CDA and DR19, which were able to react with the *N*-hydroxymethyl groups of TMM or HMM,⁸ and because of the self-condensation between the *N*-hydroxymethyl groups,⁹ samples II and III formed a crosslinking network in the process of curing/poling. Sample I, however, was a simple host/guest type without crosslinking agent and could not form a crosslinking network. Figures 3, 4, and 5 present the IR spectra of samples I, II, and III before and after curing, respectively. No difference is found between the two IR spectra in Figure 3. In Figure 4, the peaks at 3361, 1558, 1369, and 1001 cm^{-1} represent hydroxyl groups, *N*-hydroxy-

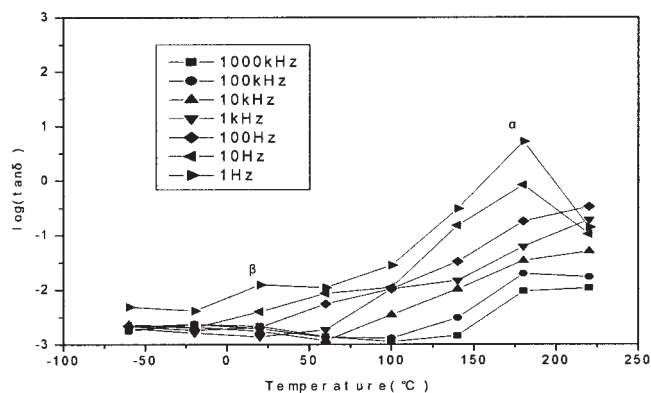


Figure 7 The temperature dependence of $\log(\tan \delta)$ for sample II.

methyl groups, *N*-hydroxyethyl groups, and primary hydroxyl groups, respectively.¹⁰ In Figure 5 the peaks at 3366, 1554, 1364, and 1003 cm^{-1} represent hydroxyl groups, *N*-hydroxymethyl groups, *N*-hydroxyethyl groups, and primary hydroxyl groups, respectively. The area of these peaks decreased after curing, suggesting their reactions in forming crosslinking networks.

The molecular chain relaxation of the samples should be hindered by the crosslinking network. Broadband dielectric spectroscopy is effective for studying the relaxation behavior of NLO polymers. The temperature dependences of the dielectric loss [$\log(\tan \delta)$] of cured samples I, II, and III are given in Figures 6, 7, and 8, respectively. The dielectric relaxation experiments were carried out under the conditions from 1 Hz to 1000 kHz and from -60 to 220°C . The relaxation of chain segments would be too late to be matchable for a higher frequency if the temperature was not high enough. Therefore, the temperature should increase to capture the relaxation of chain segments under the condition of high frequency or the frequency should be low. This means that the relax-

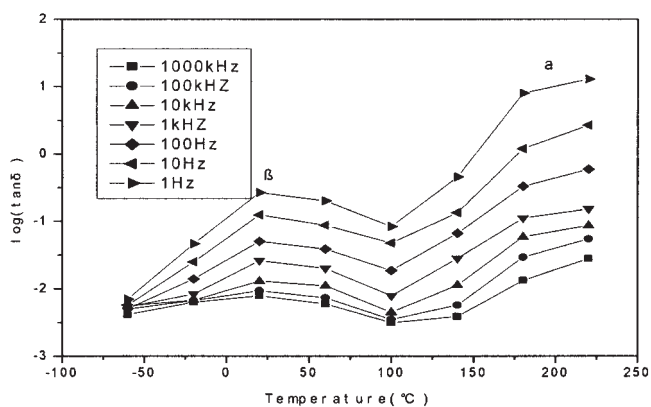


Figure 8 The temperature dependence of $\log(\tan \delta)$ for sample III.

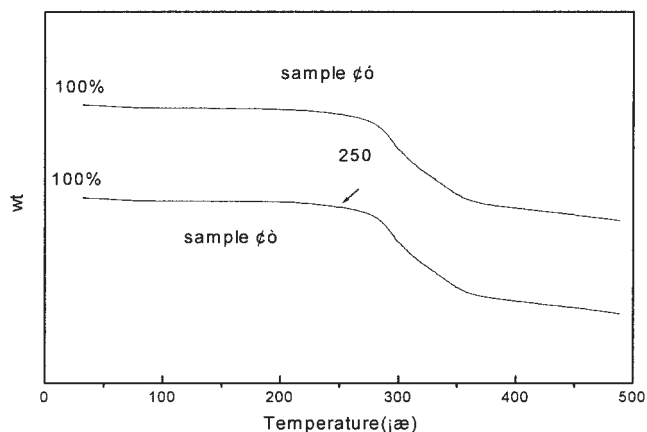


Figure 9 TGA curves of samples II and III after curing.

ation can be shown apparently at low frequency at the same temperature.¹¹ For this reason, the data at 1 Hz were used for discussion. The β relaxation, observed near 20°C at 1 Hz, is attributed to the motion of a methylene or methylene ether bridge and some unreacted groups.¹² The smaller amplitude of the β relaxation of sample II [$\log(\tan \delta) = -1.91$] compared to that of sample I (-1.64) implies the formation of a crosslinking network of sample II.¹³ However, sample III containing the HMM with six functional groups, which is more than those of TMM contained in sample II, shows only slightly higher amplitude [$\log(\tan \delta) = -0.672$] than sample I. This abnormal phenomenon might be in relation to some polar small molecules as water adsorbed by the CDA, and the stronger capillary condensation resulted from the denser crosslinking network of sample III. Such polar small molecules could result in a higher $\log(\tan \delta)$ value due to strong Maxwell-Magner surface polarization.¹⁴

The α relaxation in the figures is associated with the glass transition of the samples. The temperature of the α relaxation of sample I is about 100°C whereas those of samples II and III are about 180 and 220°C, respectively, at 1 Hz. The cured sample can contain chain segments of different lengths between crosslinking points and thus of different relaxation mobility.¹² Higher crosslinking density could restrict the mobility of chain segments and make the temperature of the α relaxation higher. The temperature of the α relaxation for samples II and III revealed their crosslinking structure. Sample III had a higher temperature of α relaxation than sample II, implying that the crosslinking density of sample III was higher than that of sample II. The temperature of α relaxation of sample I in Figure 6 is the lowest among the three samples, because it did not form any crosslinking structure. However, the $\log(\tan \delta)$ values of the α relaxation in the figures of samples II and III are slightly higher than that of sample I, which might be in relation to some unre-

acted molecules of TMM and HMM or some condensates of them, which could weaken the intermolecular force of the samples and behave similar to plasticizers.

Figure 9 shows the TGA curves of samples II and III after curing. No evident weight loss below 250°C is found, which means cured samples II and III have good heat resistance.

Transmission loss of laser

The transmission losses of the laser for samples I, II, and III were less than 0.68, 0.50, and 0.44 db, respectively, at wavelengths of 1100–1600 nm.

Electrooptic coefficient

The r_{13} value was initially determined 5 h after curing and poling (the first day in Fig. 10), and then each day thereafter. Figure 10 depicts the temporal behavior of r_{13} of the three samples at room temperature. It can be seen that the r_{13} values determined on the first day for samples I, II, and III are 0.89, 1.11, and 1.03 pm/V, respectively. The r_{13} value of sample I decreases rapidly to 0.51 pm/V after only 1 day, which is 57% of its first value. The r_{13} values of samples II and III decrease to 0.82 and 0.84 pm/V, respectively, after 4 days and stabilize at 80 and 81.5% of their initial values. It is clear that the crosslinking network hindered the orientation relaxation of the chromophores to a certain degree. In addition, sample I possessed a lower r_{13} than the others at the first day. The reason might be, more or less, in relation to the relaxation during the 5 h between the end of poling/curing and the time at which the first determination was carried out. Figure 10 proves that the relaxation of sample I is faster than the others in an earlier stage.

The thermal stability of the r_{13} of poled samples II and III was obtained by measuring the r_{13} after pol-

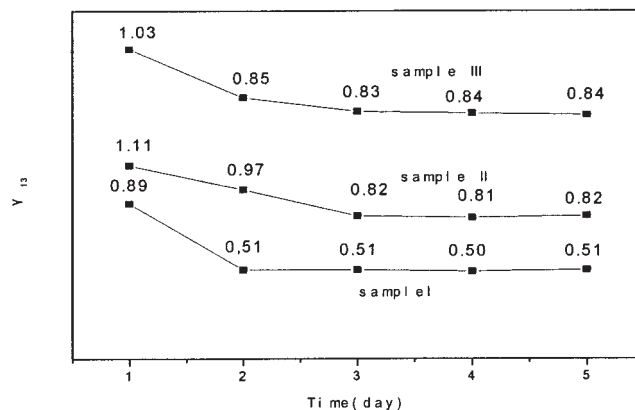


Figure 10 The temporal behavior of the electrooptic coefficient (r_{13} , pm/V) of the three samples. (Note: the value on the first day was determined at 5 h after poling/curing.)

ing/curing initially and then after keeping the samples in an oven at 100°C for 15 h. Seventy-three percent of the initial r_{13} value of sample III remained, whereas only 60% of sample II was left.

CONCLUSION

The electrooptic coefficient of the crosslinking second-order NLO materials based on CDA and melamine derivatives was 1.11 pm/V at a 1550-nm laser wavelength and a 12.7-kHz modulation frequency and decreased to 80% of its initial value after 4 days when TMM was used as the crosslinking agent. Its transmission loss of laser was 0.50 db at a laser wavelength of 1100–1600 nm. The corresponding values of the NLO material with HMM as the crosslinking agent were 1.03 pm/V, 81.5%, and 0.44 db. No evident weight loss below 250°C was found in samples II and III. The relaxation was suppressed by crosslinking, but unreacted crosslinking agent and its self-condensate could weaken the intermolecular force of the material and exert an influence on the relaxation.

References

1. Morazari, M. A.; Knoesen, S. T.; Kowel, S. T.; Higgins, B. G.; Dienes, A. *J Opt Soc Am* 1989, B6, 733.
2. Burland, D. M.; Miller, R. D.; Walsh, C. A. *Chem Rev* 1994, 94, 31.
3. Mark, H. F.; Bikales, N. M.; Overberger, C. G.; Menges, G. *Encyclopedia of Polymer Science and Engineering*; Wiley: New York, 1985; Vol. 3, p 181.
4. Brydson, J. A. *Plastics Materials*, 4th ed.; Butterworths Scientific: London, 1982; p 613.
5. Billmeyer, Jr., F. W. In *Textbook of Polymer Science*, 3rd ed.; Wiley: New York, 1984; p 441.
6. Jeng, R. J.; Hsiue, G. H.; Chen, J. I.; Marturunkakul, S.; Li, L.; Jiang, X. L.; Moody, R. A. *J Appl Polym Sci* 1995, 55, 209.
7. Hsiue, G. H.; Lee, R. H.; Jeng, R. J. *J Polym Sci Part A: Polym Chem* 1999, 37, 2503.
8. Allcock, H. R.; Lampe, F. W.; Mark, J. E. *Contemporary Polymer Chemistry*, 3rd ed.; Pearson Education Inc.: Upper Saddle River, NJ, 2003; p 49.
9. Mao, S. S. H.; Ra, Y. S.; Guo, L.; Zhang, C.; Dalton, L. R. *Chem Mater* 1998, 10, 146.
10. Huang, M. L. *Infrared Spectroscopy and Organic Molecular Structure* [in Chinese]; Science Press: Beijing, 1982; p 20.
11. Liu, F. Q.; Tan, X. Y. *Macromolecular Physics* [in Chinese]; Beijing: China University Press, 1994; p 366.
12. Hsiue, G. H.; Lee, R. H.; Jeng, R. J. *Chem Mater* 1997, 9, 883.
13. Landry, C. J. T.; Coltrain, B. K.; Brady, B. K. *Polymer* 1992, 33, 1486.
14. Hedvig, P. *Dielectric Spectroscopy of Polymers* [Chinese translation]; Akademiai Kiado: Budapest, 1977; p 286.
15. Liu, F. Q.; Tan X. Y. *Polymer Physics* [in Chinese]; Advanced Education Press: Beijing, 1995; p 379.